23. Artificial Meteor Ablation Studies

Maxwell B. Blanchard
Ames Research Center, NASA
Moffett Field, California

Artificial meteor ablation was performed on natural minerals, composed predominately of magnetite and hematite, using an arc-heated plasma stream of air. Analysis of the ablated debris indicates most was composed of two or more minerals. Wustite, a metastable mineral, was found to occur as a common product. The "magnetite" model, whose content was 80 percent magnetite, 14 percent hematite, 4 percent apatite, and 2 percent quartz, yielded ablated products consisting of over 12 different minerals. Magnetite occurred in 91 percent of all specimens examined, hematite in 16 percent, and wustite in 39 percent. The "hematite" model, whose content was 96 percent hematite and 3 percent quartz, yielded ablated products consisting of over 13 different minerals. Hematite occurred in 47 percent of all specimens examined, magnetite in 60 percent, and wustite in 28 percent. The more volatile elements (Si, P, and Cl) were depleted by a reduction of about 50 percent in the amounts present. Also, the relative abundance of Fe increased as a result of both volatile depletion (loss of Si, P, Cl, and Ca) and a reduction in its oxidation state. Hematite was converted to magnetite in the ablation zone along the model's front face. Also, quartz and apatite minerals were converted to an Fe-rich glass consisting of varying amounts of Si, P, Cl, and Ca, depending upon the accessory minerals available at the time of melting. These glass phases occurred as unusual myrmekiticlike intergrowths, which are unique textural indicators of the environment through which the material has survived. The chemistry and mineralogy of these phases remains the only trace of the original minerals. This study has shown that artificially created ablation products from iron oxides exhibit unique properties that can be used for their identification. These properties depend on the composition of the original material and the environmental conditions of formation. In addition to the accepted elemental criteria, these properties are morphologic characteristics, textural parameters, and the existence of metastable minerals.

OVER THE PAST FEW YEARS many investigators have searched for cosmic dust. They have examined particles from sediments (Marvin and Einaudi, 1967), glacial ice (Hodge et al., 1967), and the atmosphere. Atmospheric particles have been collected using aircraft (Carr, 1970), balloons (Brownlee and Hodge, 1969), and rockets (Farlow et al., 1970). In some instances, particle collections have been so sparse that long and involved analytical methods have had to be used to demonstrate even the existence of any specimens (Ferry et al., 1970, and Blanchard et al., 1968). In other instances, the abundance of particles has been overwhelming (Hemenway and Soberman, 1962). In either case, however, the basic problem was to identify the cosmic dust particles and separate them from the artificial and naturally occurring terrestrial contaminants.

Investigators have had only limited success at making positive identifications. Elemental evidence has been the main requisite to substantiate cosmic origin. The most common approach has been to examine the collection for a group of particles containing Ni. Usually occurrence of Ni in sufficient quantity to correlate with Ni-Fe meteorites, or more simply cosmic abundance, allows a case for cosmic origin to be made. Of course, possible contaminants must be ruled out first. Indeed, certain investigations (Blanchard and Farlow, 1966; Blanchard et al., 1967) have shown this latter need quite effectively. However, the relative abundance of Ni-rich particles has been small when compared with the total population. For example, less than 3 percent of spherules collected from Greenland ice contained Ni (Hodge et al., 1967). The remaining particle types are often characterized by a similar assemblage of elements but without Ni. More recently, the occurrence of Ti has been proposed to indicate a volcanic origin for Fe-rich spherules (El Goresy, 1967). Early investigations suggested the occurrence of Mn to indicate a terrestrial origin, but recent studies (El Goresy, 1967) indicate Mn has no genetic importance. At any rate, firmer criteria for identifying particles of cosmic origin are needed.

The most recent results obtained by the Smithsonian's short-lived phenomena program (Anonymous, 1970), indicate large quantities of cosmic material are reaching Earth. Results of the Prairie Network (McCrosky, 1968) have shown a frequency of fireballs perhaps two orders of magnitude greater than earlier studies. Even though large amounts of cosmic dust are reaching the Earth's surface, very little is being positively identified because Ni abundance is not an adequate criterion. More emphasis on chemistry and mineralogy is required for firm cosmic identification.

Meteors, fireballs, and micrometeoroids have one property in common: they ablate while entering the Earth's atmosphere. Micrometeoroid interaction with the atmosphere has been examined theoretically (Kornblum, 1969) and results indicate only submicron-size particles may pass through the atmosphere unaltered. Moreover, those particles in the micron size range would be nearly, if not entirely, ablated away. Larger bodies experience vaporization and fragmentation during entry. That destructive action on these larger bodies may be severe has been shown by experiments designed to study drag, ablation, and radiation effects using a constricted-arc supersonic jet to simulate meteor entry to the Earth's atmosphere (Shepard et al., 1967).

Using this unique experimental facility, it has been possible to simulate meteor ablation under controlled conditions. Initial studies (Blanchard, 1969) showed that mineral fractionation played a key role in determining the form and type of products formed. These products showed a resemblance to the parent body (Blanchard, 1970a and b) but also exhibited features characteristic of this unique environment.

Therefore, a new series of experimental studies in artificial meteor ablation has been initiated for the purpose of learning more about the reactions and products resulting from the ablation environment. This paper is the first of several that will present results of artificial ablation experiments performed on synthetic and natural materials designed to determine those features occurring in naturally ablated products characteristic (or nearly so) of the ablation environment.

PROCEDURE

The models used for these experiments were "magnetite" and "hematite," each with accessory minerals. The facility used for these artificial meteor ablation experiments was a constricted-arc supersonic jet (fig. 1). Operation of the arc jet requires a potential difference of about 1 kV between the tungsten cathode and multiple anode; a current of about 100 A is used. A plasma is generated that flows from the cathode toward the anode, consisting of: electrons, a small amount of argon used to bathe the cathode to reduce its oxidation rate, and high-pressure air ionized to simulate the Earth's atmosphere through which the artificial meteor is traveling. By matching the chamber pressure and the nozzle exit pressure the plasma stream is focused into a near-parallel shaped beam. Facility conditions established for these experiments simulate a low velocity meteor traveling about 12 km/s at an altitude of 70 km.

A pan-shaped copper collector, with a water-cooled jacket to prevent melting, was precleaned and placed inside the chamber. The model to be
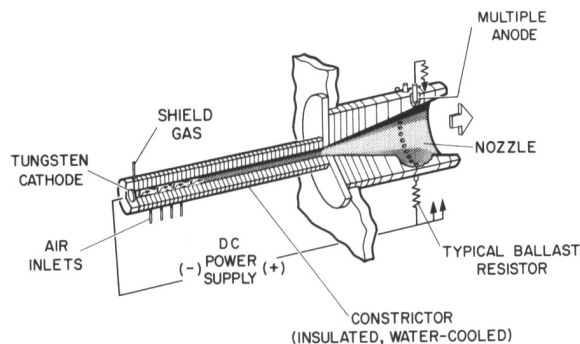
FIGURE 1.—Schematic drawing of a constricted-arc supersonic jet.

ablated was mounted facing the arc jet on a hollow rod cooled by water circulating within it. The model was moved by a servomechanism into the plasma beam after the beam was focused. The entire period of ablation usually lasted no more than 30 s. Generally, about 90 percent of the ablated material was recovered on the collector and chamber floor. The remaining material, distributed throughout the tunnel, was too contaminated for analytical use.

Material recovered from the chamber floor was sorted from any obvious contaminants. Despite attempts to minimize contamination by precleaning the chamber with a vacuum cleaner and repeated washings with distilled water and absorbent paper towels, small chips from screws, bolts, and other sources were occasionally found. However, all material on the collector was contaminant free. This latter material was immediately recovered after the experiment and returned to a cleanroom where the debris was removed from the collector using a brush and a strong pressure rinse with trifluorotrichloroethane. The material was flushed into filtering apparatus and finally recovered on a membrane filter. This procedure prevented contamination in the particle size range below 1 mm.

Optical microscopy studies were performed using the stereo microscope by subdividing the material into groups based on particle morphology. Each group was weighed and counted. Representative numbers of particles from each group were selected for analysis. Analyses were performed using a metallurgical microscope, x-ray diffraction/fluorescence and an electron microprobe. For all analyses, the original model, the ablated front face, and the debris collected were compared. Metallurgical microscopy studies consisted of viewing polished specimens with bright- and dark-field incident light to examine textures and identify phases. Only a few samples of each particle group were examined in this manner. X-ray fluorescence studies consisted of determining relative abundance of the principal elemental constituents in the models for making comparisons with the collected debris. Bulk samples were examined to detect changes in abundance of volatile elements.

The principal analytical method for identifying the many iron oxide phases was x-ray diffraction which easily and reliably separates all of the iron oxide minerals. Over 1000 individual particles ranging from 10 μ to 700 μ were analyzed. Specimens were mounted on this glass rods and positioned inside 57.3-mm-diameter Debye-Scherrer cameras. Exposure periods ranged from 12 to 24 hr using Ilford-G film. All cameras were purged with helium gas during the exposure period to minimize background from air scatter. Identifications were made using film overlays similar to that shown in figure 2. Data for all suspected minerals were taken from ASTM cards and converted into Debye-Scherrer film format on a stable base drafting medium. Phototransparencies were then made with six separate patterns on each transparent overlay. Most of the particles contained two or more minerals; these particles were identified by visually subtracting the diffraction pattern for each major constituent in the film, leaving the most intense lines from minerals remaining to be matched again.

Electron microprobe studies using the MAC Model 400 were performed on the original model and on the ablation zone along the model's front face. Over 100 individual grains of each mineral present in the model were qualitatively analyzed with an energy dispersive, silicon detector and a multichannel pulse height analyzer. Grains in the model and those in the ablated zone along the frontal face were then compared for elemental homogeneity.

Quantitative analyses were performed with spectrometers having either a sealed proportional detector using a LiF crystal, or a flow proportional detector using an ADP or PET crystal depending on the wavelength and peak-to-background ratio
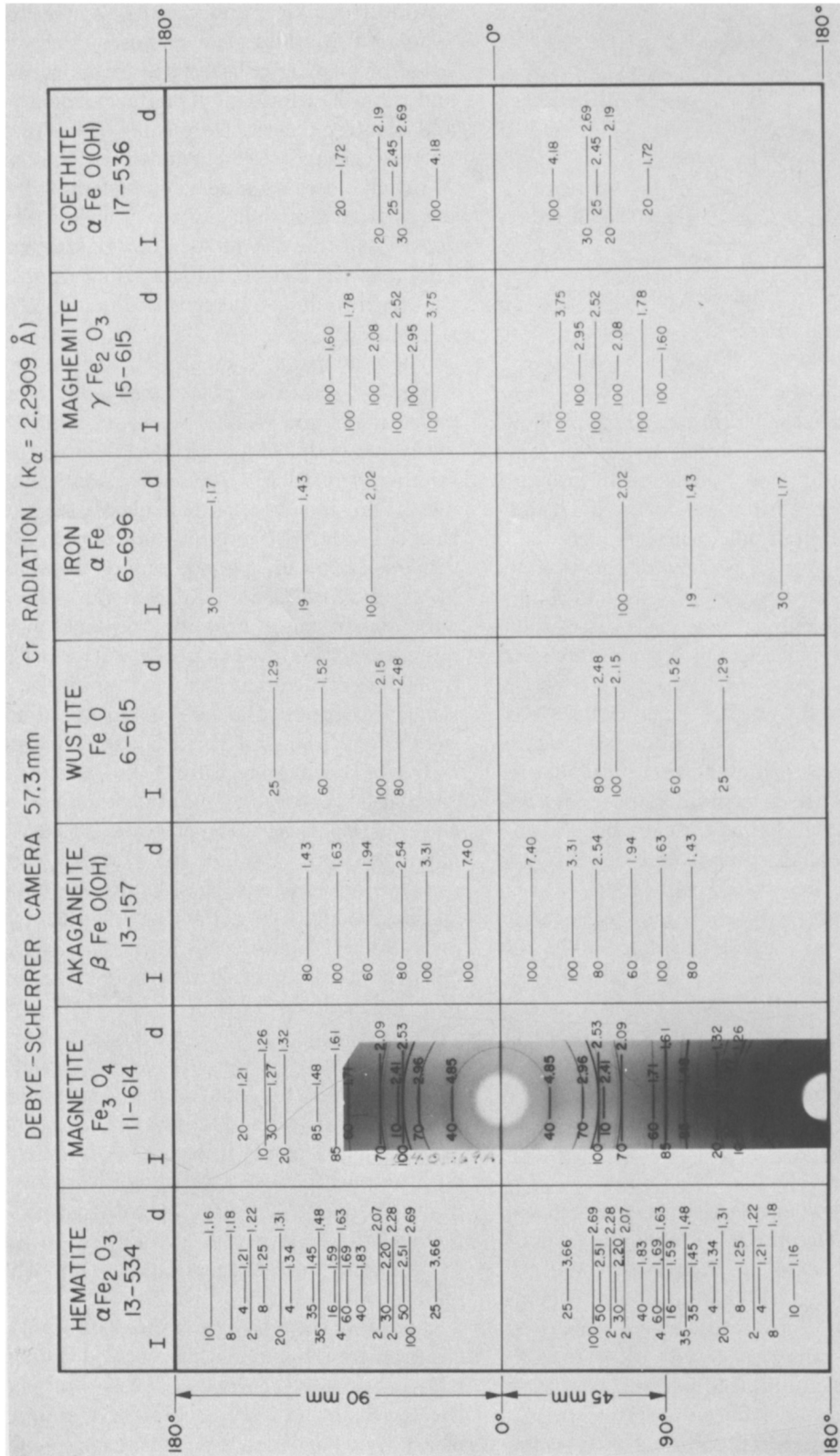
FIGURE 2.—X-ray diffraction film overlay.

required. All analyses were conducted with an accelerating potential of 25 kV. Specimen current for qualitative analysis using the energy-dispersive detector was usually 0.0100 μA. For quantitative analysis using the crystal spectrometers it ranged between 0.0050 and 0.0100 μA, depending on the nature of the grain to be analyzed. Corrections for drift, background, and detector dead time were applied to all data. Absorption corrections were made using the method outlined by Adler and Goldstein (1965). Heinrich's (1966) mass absorption values were used in this procedure. X-ray fluorescence corrections were made using Colby's (1966) procedure. Atomic number corrections were made according to Thomas's (1964) procedure.

RESULTS AND DISCUSSION

Optical Studies

Particles found on the collector were subdivided into groups on the basis of their morphology. Figure 3 illustrates the particle groups; their descriptions are given in table 1. Groups C and D represent those particles not readily exhibiting characteristics of melted products and substantiate that at least a certain part of the ablated debris does not look like melted products. For these experiments, this portion of the debris represented 20 percent by weight of all collected products. A histogram of the collected debris from the "magnetite" ablation experiment showing its weight percent and the quantity of particles in each group is shown in figure 4. The distribution of particle groups and their relative amounts compares favorably for both "hematite" and "magnetite" models even though the amount of "hematite" ablated was less than 10 percent of the amount of "magnetite" ablated. A frequency size distribution was made for the group X particles (fig. 5). This positively skewed distribution indicates the bulk of the small particle debris centers about a median value of 354 μ. However, there is a sizable quantity of debris generated by the ablation process in the size range down to 2 or 3 μ. Smaller particles probably exist but are not collected because they remain in the plasma beam and are evenly dispersed throughout the chamber. A quantity of particles in the 1 to 100 μ size range were recovered on membrane filters and showed a

great diversity of colors, e.g., yellow, red, orange, clear, milky. Because many of these also appear in particle collections taken with the plasma beam operating but without a model ablating, most are probably contaminants from the facility. However, many molten particles as small as a few microns in size struck larger bodies already solidified on the collector leaving splatter marks on the surface of the larger bodies (fig. 6).

X-Ray Diffraction Studies

X-ray diffraction analysis of approximately 1000 individual ablated specimens was performed. Particle sizes ranged from 10 to 700 μ. Selected specimens from each morphologic group were examined in numbers proportional to the amount present in each group. Those selected were judged to be most typical for that group, although an unusual specimen was almost always examined. Because most of the specimens analyzed contained two or more minerals the diffraction patterns were complex. Development of the film overlay technique, using actual ASTM file data converting d values into measurements drawn on transparent films, allowed rapid identifications for most of the diffraction patterns. Table 2 shows the magnetite data compiled from 614 patterns, of which 59 percent contained two or more minerals. The "magnetite" mineral model was composed of 80 percent magnetite, 14 percent hematite, 4 percent apatite, and 2 percent quartz. The hematite occurred interstitially between euhedral magnetite grains. Over 12 different minerals were recognized in the ablation products. Note that the frequency of occurrence given cannot be compared with percent abundance. Magnetite, for example, will be somewhat less in abundance than the 91 percent frequency of occurrence suggests because it occurred alone, as a major constituent mixed with other minerals, and occasionally as a minor constituent. Hematite and wustite will be considerably less in abundance than the 16 percent and 39 percent listed because they occurred almost exclusively as minor constituents. Hematite occurred alone only occasionally and wustite only rarely. Nearly all the wustite identified was based on the four most intense d spacings; only two patterns had five (all that can be recorded on film using Cr radiation) of the eight lines listed on the ASTM card. All of
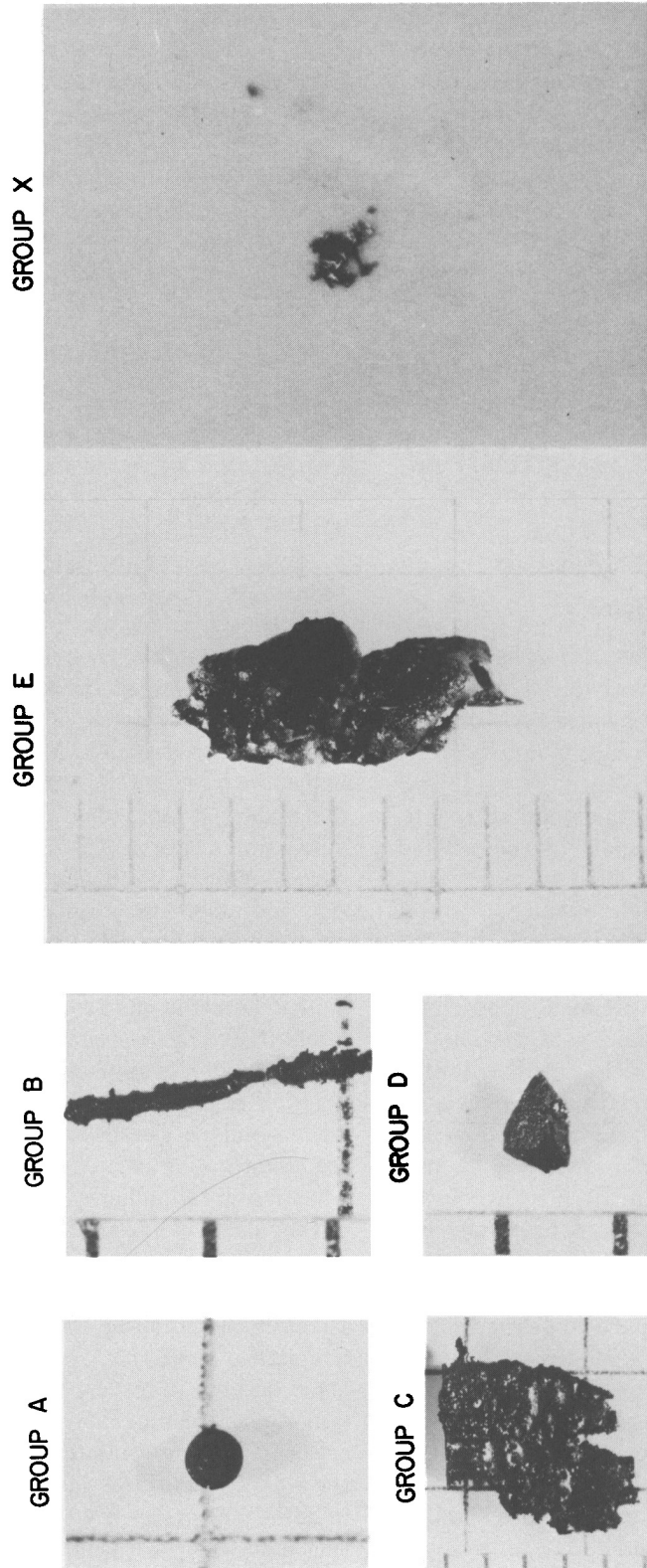
FIGURE 3.—Illustration of particle groups collected from ablation experiment.

TABLE 1.—*Characteristics of Particle Groups Collected From Ablation Experiment*

Group	Shape	Color	Texture
A	Spheres, spheroids, flattened spheroids; many have protuberances.	*Fresh*—silver *Oxidized*—red brown, brown, copper, gold, blue, purple, gray, black	Dull lusterless finish on red brown and gray particles; metallic colors have shiny surface but are not often smooth; general surface appears grainy, some are rough and scaley; many show voids; some are hollow.
B	Flattened droplets and elongated pieces; length-to-width-ratio >5.	*Fresh*—silver *Oxidized*—red brown, brown, copper, blue, gold, gray, black	Dull lusterless finish on red brown and gray particles; metallic colors have shiny surface but are not often smooth; surface appears grainy; some particles are very rough and show discrete octahedrons; many voids at surface.
C	Platelike, very thin flat chips generally equant or rectangular outlines.	*Fresh*—silver *Oxidized*—red brown, brown, copper, blue, gray, black	Dull lusterless on red brown and gray particles; metallic colors have a shiny surface but are not smooth; some show discrete octahedrons; many have very small (<10 μ) flattened droplets on the top surface.
D	Pyramidal, tabular, equant blocks and granules; no more than one side shows melted surface; most easily distinguished by angular edges and broken sides; collector shaped surface and melted surfaces are not readily recognized.	Almost all have fresh surfaces that yield a shiny silver and black color; only occasionally are oxidized surfaces found.	Characterized by freshly broken edges and sides; all particles have angular appearance; voids occur.
E	Irregular or ropy bodies; shape controlled by collector; melted surfaces immediately recognized; length-to-width ratio >2 or 3; some have octahedral crystals at surface.	Fresh edges are shiny silver or black, collector shaped sides are shiny gray, sometimes blue or gold; melted surface ranges in color from dull red brown to shiny gold, silver, or gray.	Sharp pointed edges and grainy surface features; voids are dominant; octahedral crystals are common.
X	Pyramidal, tabular, granular, platelike chips, flattened droplets, and spherules; all particles smaller than 1 mm.	Yellow, red, orange, clear, milky, amber, gray, black, silver.	Ranges from freshly broken edges and sides to shiny smooth surfaces.

the hematite identified had four or more of the most intense lines. Most of the time eight or more lines were present. Magnetite's identification was almost always based on the presence of 12 or more lines in the diffraction pattern. Patterns that were not identified usually could be divided into about five separate mineral groups based on pattern similarities.

An attempt was made to correlate mineral content of the particles with earlier recognized morphologic groups (fig. 3 and table 1). Results are shown in table 3 for the "magnetite" model.

Note that all groups (even those not readily exhibiting signs of having been melted) reflect about the same frequency of occurrence for magnetite, hematite, and wustite. This characteristic suggests that mineralogical trends can be established from a smaller quantity of samples and even by restricting the specimens to one particle group. Lepidocrocite appears only in irregular-shaped particles, whereas goethite appears only in particles resembling thin platelike chips. Perhaps this association can be best explained by the uniqueness of the particle groups in that they both
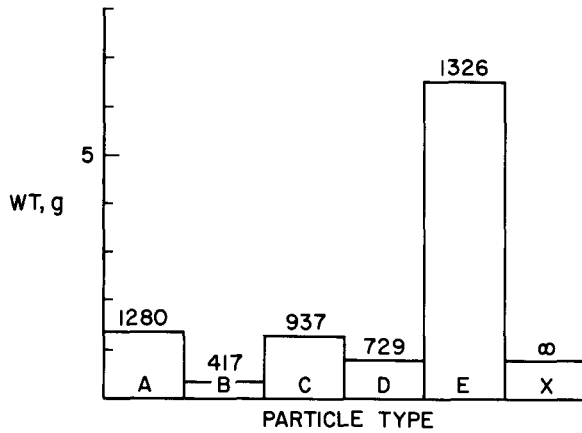
SAMPLE X = ALL PARTICLES SMALLER THAN 1mm
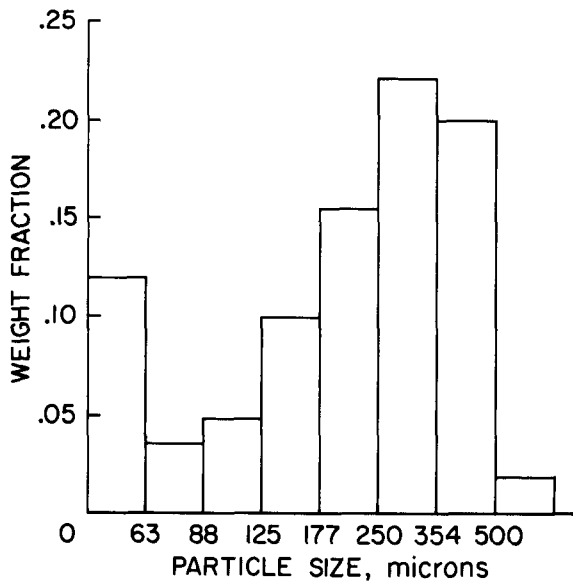
FIGURE 4.—Collected debris from magnetite model.

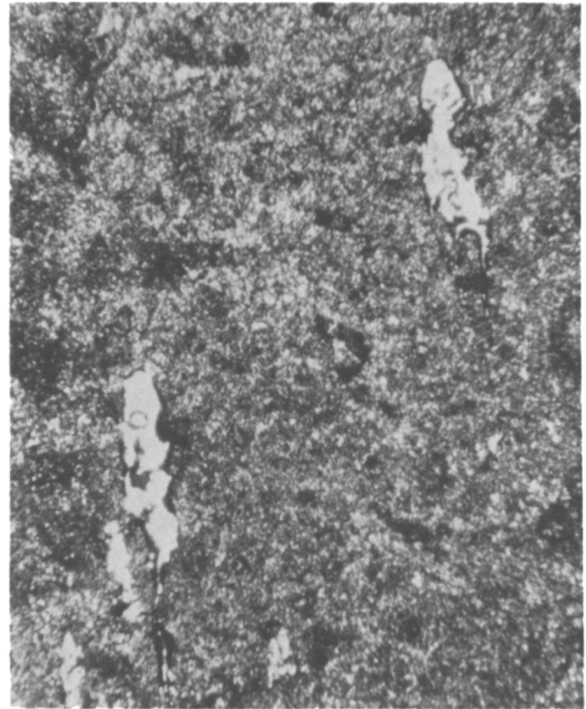FIGURE 5.—Frequency size distribution of group *X* particles.

FIGURE 6.—Flattened droplet with micron size splatter drops.

as a few small individual octahedral crystals in a porous matrix of hematite. Over 13 different minerals were recognized in the ablation products. These minerals were identified in a manner similar to that for the "magnetite" model. The most significant difference noted was the reduction in the amount of hematite present and, at the same time, a dramatic increase in the amount of magnetite and wustite present in the products. As before, the existence of unidentified patterns suggest about five minerals may be represented. The occurrence of akaganeite, lepidocrocite, and goethite are believed to be post ablation alteration products probably from magnetite. Copper particles encountered came from the collector or facility chamber parts. Aluminum particles originated from a pan used to cover the collector during transit.

X-Ray Fluorescence

Analyses were conducted on bulk powdered samples from the model and ablated products. These studies were performed to correlate the "be-

have an unusually high ratio of surface area to volume, which favors the formation of alteration products.

With the foregoing results in mind, an examination of hematite ablation products was performed. However, a lower quantity of specimens was examined: 181 particles were analyzed, of which 56 percent contained two or more minerals. Table 4 gives data from the hematite analysis. The model was composed of 96 percent hematite, 3 percent quartz with some magnetite. Magnetite occurred

TABLE 2.—*X-Ray Diffraction Analysis of Ablation Products From "Magnetite" Model*

Mineral	Occurrence [a]		Percent frequency of occurrence
	Major constituent	Minor constituent	
Magnetite	549	12	91
Hematite	5	94	16
Wustite	2	236	39
Lepidocrocite	2		<1
Goethite	1		<1
Unknown (≈5 different patterns)	20	1	3
Copper contaminant	15		2
Aluminum contaminant	2		<1

[a] Total number of particles analyzed: 614.
  41% patterns with one mineral
  59% patterns with two or more minerals

TABLE 4.—*X-Ray Diffraction Analysis of Ablation Products From "Hematite" Model*

Mineral	Occurrence [a]		Percent frequency of occurrence
	Major constituent	Minor constituent	
Hematite	67	18	47
Magnetite	84	25	60
Wustite	2	49	28
Akaganeite	3	4	4
Lepidocrocite	1	1	1
Goethite	2	1	1
Unknown (≈5 different patterns)	9	1	6
Copper contaminant	3	4	4
Aluminum contaminant	10	1	6

[a] Total number of particles analyzed: 181.
  44% patterns with one mineral
  56% patterns with two or more minerals

TABLE 3.—*Comparison of Particle Shape With Mineral Content of Ablated Products From "Magnetite" Model*

Shape	Number analyzed	Percent frequency of occurrence					
		Magnetite	Hematite	Wustite	Lepidocrocite	Goethite	Unknown
Spherules	142	98	24	37			1
Flattened particles	87	96	17	36			3
Thin plate-like chips	13	85	15	38		8	
Granules	168	99	11	43			3
Irregular bodies	173	96	13	45	1		6
Total	583						

fore" and "after" chemistry. Earlier experiments (Walters and Giutronich, 1967) have demonstrated that vapor fractionation can seriously affect the end products by depleting certain more volatile elements. The role of vapor fractionation in the formation of the ablation products was indicated by analysis of powdered samples of the model and products. As shown in table 5 the elements Si, P, and Cl show strong evidence of volatile depletion by about 50 percent reduction in amounts present. The element Ca shows an apparent depletion of 20 percent of the amount present. An increase in the relative abundance of Fe is a result of both volatile depletion and a reduction in its oxidation state. This last feature is discussed in more detail later.

Electron Microprobe Analysis

Electron microprobe analyses were performed on the "magnetite" and "hematite" models and along the ablated portion on their front faces. Figure 7 is a photomicrograph of a polished surface for these models. In the "magnetite" model, magnetite occurs as euhedral grains with hematite occurring principally at grain boundaries. Sub-

TABLE 5.—*X-Ray Fluorescence Analyses*

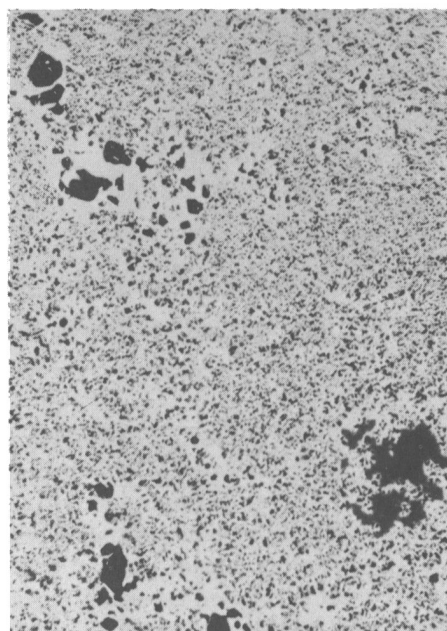| Sample	Principal elemental constituents (weight percent)				
	Si	P	Cl	Ca	Fe
Magnetite model "B"	2.4±0.5	1.1±0.2	0.3±0.1	1.6±0.3	61.0±2.0
Magnetite ablated "B"	1.2±0.1	0.5±0.1	0.1±0.1	1.3±0.2	77.5±1.0
Hematite model	1.8±0.3				63.7±1.6
Hematite ablated	1.6±0.1				68.5±0.6
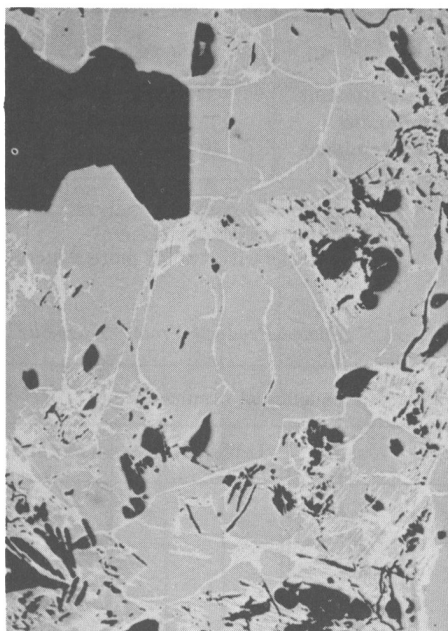
"MAGNETITE" MODEL   "HEMATITE" MODEL

FIGURE 7.—Polished sections of "magnetite" and "hematite" models.

hedral grains of apatite and anhedral grains of quartz are encountered occasionally. For the "hematite" model, magnetite occurs as very few euhedral grains isolated in a porous groundmass of microcrystalline hematite. Occasionally anhedral grains of quartz are encountered. Table 6 reports results of the analysis for the principal elements in each mineral. For these analyses, over 10 different grains of each mineral were analyzed quantitatively for the elements listed. Many more grains were analyzed using an energy dispersive detector to ensure the homogeneity of each mineral.

Analyses of the ablated zone on the front face of the "magnetite" model revealed several features;

among them is the apparent conversion of all hematite to magnetite in this zone and in a melt zone extending a few hundred microns deep beneath this surface. New products here are the result of chemical reactions occurring in the gas cap on the front face of the model. These newly formed products from the "magnetite" model are illustrated in figure 8. In the upper left-hand corner the original minerals are seen; magnetite, hematite at the grain boundaries, and one rather large grain of apatite are evident. In the central portion of the figure the hematite has been converted to magnetite, which is the only conspicuous difference. Obviously, this zone reached a molten

TABLE 6.—*Electron Microprobe Analysis of Mineral Grains in Hematite and Magnetite Models and Their Ablated Products*

Sample	Principal elemental constituents (weight percent)				
	Si	P	Cl	Ca	Fe
Magnetite model					
Magnetite	0.3±0.1	0.0	0.0	0.0	71.5±0.4
Hematite	0.0	0.0	0.0	0.0	70.0±0.3
Apatite	0.2±0.1	19.4±0.3	1.5±0.4	39.4±0.4	0.0
Quartz	46.2±0.3				0.4±0.1
Magnetite ablated zone					
Magnetite	0.0	0.0	0.0	0.0	72.2±0.3
Intergrowths	12.4 to	1.8 to	0.0 to	4.8 to	34.3 to
	14.8±0.2	2.0±0.2	0.3±0.2	7.7±0.2	44.6±1.4
Hematite model					
Hematite	0.2±0.1				70.1±0.3
Quartz	47.4±0.4				0.4±0.2
Hematite ablated zone					
Magnetite	0.0				72.6±0.2
Intergrowths	15.0 to				49.4 to
	16.04±0.5				53.1±1.9

state and in a reducing environment which explains the absence of hematite. In the right-hand portion magnetite occurs with unusual myrmekiticlike intergrowths, which exhibit planar features running generally parallel to the original orientation of the model's front face. Often the intergrowths themselves are aligned parallel with one another but perpendicular to the planar features. Electron probe studies have shown these intergrowths consist of the same elements but in different proportions. More quantitative studies showed the composition range to be 12.4 to 14.8 percent Si, 1.8 to 2.0 percent P, 0.0 to 0.3 percent Cl, 4.8 to 7.7 percent Ca, 34.3 to 44.6 percent Fe, and 33.2 to 41.4 percent O. Oxygen content was determined by subtracting the sum of all components from 100 percent. The Si, P, Cl, and Ca for this new phase came from quartz and apatite minerals occurring in the "magnetite" model. Local differences in the overall abundance of apatite and quartz from place-to-place within the model yielded compositions which vary in abundance of Si, P, Cl, and Ca.

An illustration of newly formed products from the "hematite" model is shown in figure 9. In the upper left-hand side, the original mineral hematite is seen. In the central section, the hematite has been converted to magnetite. However, original surface textures are generally preserved from the hematite through this zone of magnetite. Obviously, this zone has reached a molten state and in a reducing environment, which explains the absence of any hematite. In the right-hand portion, magnetite again occurs with myrmekiticlike intergrowths similar to those of the "magnetite" model. However, electron probe studies revealed a different composition: 15.1 to 16.4 percent Si, 49.4 to 53.1 percent Fe, and 31.9 to 34.2 percent O. This change in content results from the presence of quartz (and the lack of apatite) in the "hematite" model. Silicon for this phase came from the quartz.

X-ray diffraction Debye-Scherrer powder patterns were taken of several pieces of this intergrowth material chipped from the edge of a polished specimen, and yielded no pattern, suggesting the material was amorphous. This phase is considered to be an Fe-rich glass with varying amounts of Si, P, Cl, and Ca depending on the availability of accessory minerals in the model at the time of melting. Clearly, these intergrowths are a unique textural indicator of the environment through which the material has survived, and the chemistry and mineralogy of these phases remains the only trace of the original minerals.

ENTIRE MELT ZONE

MODEL A   MOLTEN B   ABLATED C
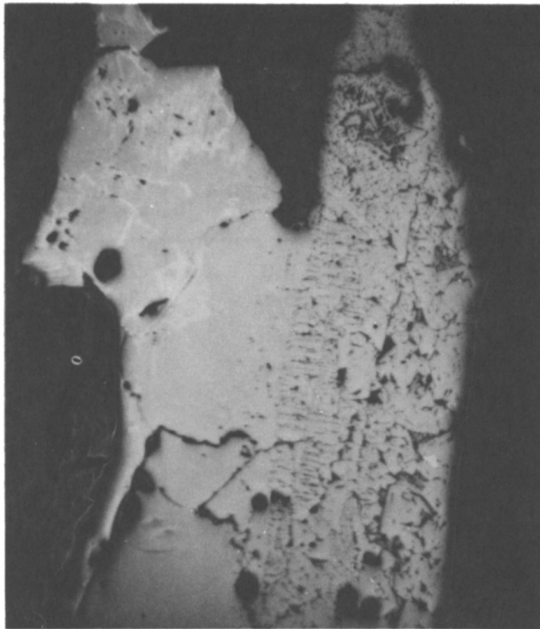
A-ORIGINAL MODEL, WITH
    MAGNETITE AND HEMATITE

B-MOLTEN ZONE, MAGNETITE ONLY,
    ORIGINAL TEXTURES PRESERVED

C-ABLATED ZONE, SHOWING
    MAGNETITE MYRMEKITIC-LIKE
    INTERGROWTHS COMPOSED OF
    Si, P, Cl, Ca, Fe AND O

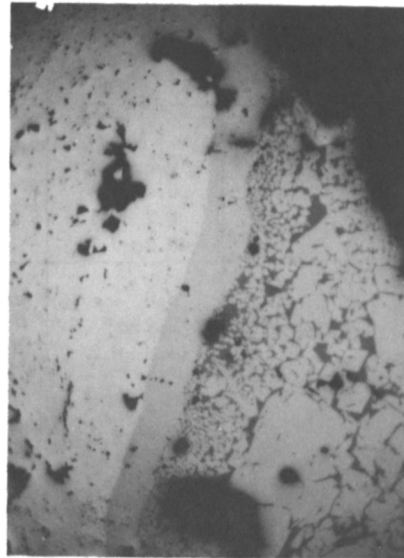FIGURE 8.—Magnetite ablated model.

CONCLUDING REMARKS

This study has shown that artificially created ablation products from iron oxides exhibit unique properties that can be used for identification. These properties depend on the composition of the original material and the environmental conditions of formation. In addition to the accepted elemental criteria, these properties are: morphologic characteristics, textural parameters, and the existence of metastable minerals.

Elemental criteria have been effectively used in

ENTIRE MELT ZONE

MODEL A   MOLTEN B

                 ABLATED C

A-ORIGINAL MODEL, WITH HEMATITE

B-MOLTEN ZONE, MAGNETITE ONLY,
    ORIGINAL TEXTURES PRESERVED

C-ABLATED ZONE, SHOWING
    MAGNETITE PLUS MYRMEKITIC-
    LIKE INTERGROWTHS COMPOSED
    OF Si, Fe AND O

FIGURE 9.—Hematite ablated model.

a recent investigation of debris collected by aircraft from the Revelstoke and Allende events (Carr, 1970). However, the largest particle size of this material was less than the minimum size examined in this study so application of the proposed properties will have to await further collections.

Morphological characteristics recognized in this study included spherules, flattened droplets, elongated particles, and irregular or ropy bodies with vesicular features. A considerable portion of the debris found in this study was so fragile that many pieces less than 1000 μ in size did not even appear as melted products, yet x-ray diffraction studies clearly showed that all were indeed melted products.

Textural parameters recognized in this study are the existence of myrmekiticlike intergrowths

indicative of the ablation environment. Moreover, the elemental content of these glassy intergrowths offers the only real clues to the initial mineral content of the original body. Serious problems exist in extrapolating back to original mineral content using these phases because certain more volatile elements have been depleted.

Formation of a metastable mineral, wustite, occurred in this study. Wustite was only found in particles less than 1000 μ in size. Particles in this size range radiate heat sufficiently fast to produce a quenching condition, which is responsible for preserving the wustite.

The ablation facility simulated a meteor traveling approximately 12 km/s at an altitude of 70 km. At this altitude, the oxygen partial pressure is about 10^{-2} mm. In contrast, the partial pressure of oxygen at sea level is about 160 mm. Indications are the oxygen partial pressure may reach a maximum as high as 16 mm but only for a short time in the gas cap on the model's front face. While this environment oxidizes metallic iron, it reduces Fe_2O_3. Therefore, an upper limit is clearly indicated for the oxygen available to produce a reaction with the ablating material. Moreover, there is evidence that molecular bound oxygen is lost from the hematite as revealed by mass spectrometry measurements (Ferry, 1970). This loss of oxygen together with rapid cooling explains the formation of wustite from both "magnetite" and "hematite" models. Loss of oxygen is also responsible for formation of magnetite from the "hematite" model. A temperature composition diagram for the iron-oxygen system (Darken and Gurry, 1946) shows that α iron and magnetite would be the normal expected products if wustite was not preserved by rapid cooling (fig. 10).

Formation of wustite during meteor ablation, and akaganeite, lepidocrocite, and goethite during later alteration, has been recognized for some time in meteorite fusion crusts. Wustite and akaganeite were also found in the fusion crust of the Sputnik IV fragment (Marvin, 1963). Spherules of wustite have also been found associated with other material of suspected extraterrestrial origin (high nickel/iron ratio) from ancient (Marvin and
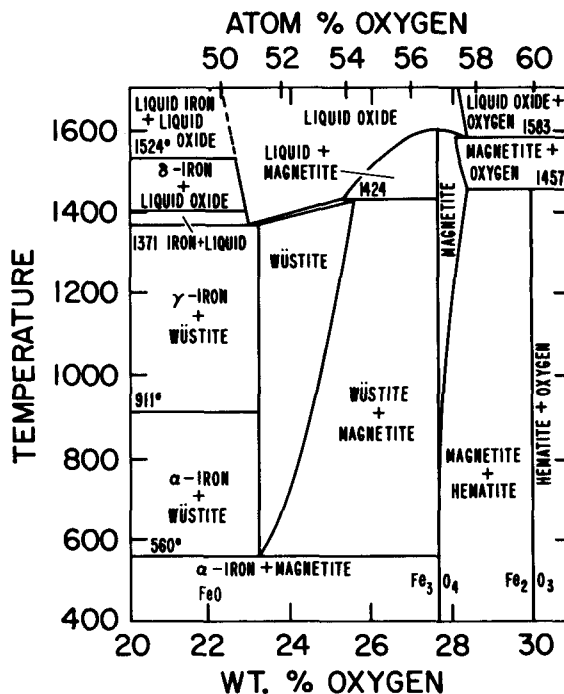

FIGURE 10.—Iron-oxygen system at a total oxygen pressure of one atmosphere; temperature-composition phase diagram. From Darken and Gurry, 1946. Iron-oxygen equilibria involving liquid oxide, *J. Amer. Chem. Soc.*, 68: 799.

Einaudi, 1968) and marine (Millard and Finkelman, 1970) sediments. Assuming industrial contaminants have been ruled out, it appears the existence of wustite and its association with other iron oxides can be used as firm criteria in identifying debris ablated from meteors and fireballs.

ACKNOWLEDGMENTS

REFERENCES

ADLER, I., AND GOLDSTEIN, J., 1965. Absorption tables for electron probe microanalysis, *NASA Tech. Note* **D-2984,** 267.

ANON., 1970. Annual report, 1969: Smithsonian Institution—center for short lived phenomena, Cambridge, Mass., 246 pp.

BLANCHARD, M. B., 1970a. Artificial meteor ablation studies of iron oxide minerals, *EOS-Trans. Amer. Geophys. Union*, **51,** 831.

——, 1970b. Wustite—a common occurrence in artificial meteor ablation products, *Meteoritics*, **5,** 181.

——, 1969. Preliminary results of artificial meteor ablation (abstract), *Meteoritics*, **4,** 261.

BLANCHARD, M. B., FERRY, G. V., AND FARLOW, N. H., 1968. Analyses of particles on surfaces exposed to the 1965 Leonid meteor shower by the Luster sounding rocket. *J. Geophys. Res.*, **73,** 6347-6360.

BLANCHARD, M. B., FARLOW, N. H., FERRY, G. V., AND SHADE, H. D., 1967. Contaminants vs micrometeorites from the 1965 Leonid meteor shower, *Proc. Amer. Assoc. Contam. Contr.*, 139-145.

BLANCHARD, M. B., AND FARLOW, N. H., 1966. Contamination control during designing, fabrication, test, and launch of an upper atmosphere rocket payload, *J. Contam. Contr.*, **5,** 22-25.

BROWNLEE, D. E., AND HODGE, P. W., 1969. Results of a large volume micrometeorite collection at an altitude of 115,000 feet (abstract), *Meteoritics*, **4,** 264.

CARR, M. H., 1970. Atmospheric collection of debris from the Revelstoke and Allende fireballs, *Geochim. Cosmochim. Acta*, **64,** 689-700.

COLBY, J. W., 1966. The applicability of theoretically calculated intensity corrections in microprobe analysis, in *The Electron Microprobe*, edited by McKinley, Heinrich, and Wittry, J. Wiley and Sons, 95-188.

DARKEN, L. S., AND GURRY, R. W., 1946. The system iron-oxygen, II equilibrium and thermodynamics of liquid oxide and other phases, *J. Amer. Chem. Soc.*, **68,** 748-816.

EL GORESY, A., 1967. Electron microprobe analysis and microscopic study of polished surfaces of magnetic spherules and grains collected from the Greenland Ice, *Smithson. Astrophys. Obs., Spec. Rept.* No. 251.

FARLOW, N. H., FERRY, G. V., AND BLANCHARD, M. B., 1970. Examination of surfaces exposed to a noctilucent cloud, Aug. 1, 1968, *J. Geophys. Res.*, **75,** 6736-6750.

FERRY, G. V., BLANCHARD, M. B., AND FARLOW, N. H., 1970. Microparticle collection experiments during the 1966 Orionid and Leonid meteor showers, *J. Geophys. Res.*, **75,** 859-870.

FERRY, G. V., 1970. Preliminary interpretation of mass spectra from artificial meteor ablation, *Meteoritics*, **5,** 196-197.

HEINRICH, K. F. J., 1966. X-ray absorption uncertainty, in *The Electron Microprobe* edited by McKinely, Heinrich and Wittry, J. Wiley and Sons, 296-377.

HEMENWAY, C. L., AND SOBERMAN, R. K., 1962. Studies of micrometeorites obtained from a recoverable sounding rocket, *Astron. J.*, **67,** 256-266.

HODGE, P. W., WRIGHT, F. W., AND LANGWAY, C. C., 1967. Studies of particles for extraterrestrial origin 5, compositions of the interiors of spherules from Arctic and Antarctic ice deposits, *J. Geophys. Res.*, **72,** 1404-1406.

KORNBLUM, J. J., 1969. Micrometeoroid interactions with the atmosphere, *J. Geophys. Res.*, **74,** 1893-1970.

MARVIN, U. B., 1963. Mineralogy of the oxidation products of the Sputnik 4 fragment and of iron meteorites, *J. Geophys. Res.*, **68,** 5059-5068.

MARVIN, U. B., and EINAUDI, M. T., 1967. Black, magnetic spherules from Pleistocene and recent beach sands, *Geochim. Cosmochim. Acta*, **31,** 1871-1884.

McCROSKY, R. E., 1968. The distribution of magnitudes, masses, and energies of large meteoritic bodies, *Smithson. Astrophys. Obs. Spec. Rept.* No. 280.

MILLARD, H. T., AND FINKELMAN, R. B., 1970. Chemical and mineralogical compositions of cosmic and terrestrial spherules from a marine sediment, *J. Geophys. Res.*, **75,** 2125-2135.

SHEPARD, C. E., VORREITER, J. W., STINE, H. A., AND WINOVICH, W., 1967. A study of artificial meteors as ablators, *NASA Tech. Note* **D-3740.**

THOMAS, P. M., 1964. A method for correcting for atomic number effects in electron-probe microanalysis, *United Kingdom Atomic Energy Authority, Res. Group Rept.* No. AERE-R4593.

WALTERS, L. S., AND GIUTRONICH, J. E., 1967. Vapor fractionation of silicate melts at high temperatures and atmospheric pressures, *Solar Energy*, **XI,** 163-169.